ED-FreEst: Event-Driven Frequency Estimation

Ruiming Guo and Ayush Bhandari
Dept. of Electrical and Electronic Engg., Imperial College London, SW7 2AZ, UK.
ruiming.guo@imperial.ac.uk • a.bhandari@imperial.ac.uk

***Abstract*—Event-driven or Time-encoded sampling is an alternative to the conventional uniform sampling paradigm that encodes the amplitude information of a continuous-time signal into a sequence of time stamps. The data-driven approach of event-driven acquisition provides significant power efficiency advantages, as it initiates sampling exclusively upon the detection of specific events, such as amplitude changes. In recent years, the focus of event-driven sampling has shifted from bandlimited function classes to time-domain sparse signals. That said, the case of Fourier-domain sparse signals (frequency or spectral estimation problem) remains open. In this paper, we introduce a novel method for off-the-grid, event-driven frequency estimation (`ED-FreEst`). Empirically, our algorithm results in a lower sampling rate while offering robustness. These aspects seamlessly translate into real-world validation. To demonstrate this, we build an event-driven sampling hardware utilizing asynchronous sigma-delta modulators, showcasing the practical utility and effectiveness of our method in tangible applications.**

***Index Terms*—Event-driven, nonuniform sampling, frequency estimation, time-encoded sampling.**

I. Introduction

A fundamental question in digital acquisition is how to represent a continuous-time signal as a discrete sequence. Underpinning the prevalent digitalization technology, the Shannon-Nyquist sampling scheme [1] represents a bandlimited signal based on its amplitude samples taken at or above the Nyquist rate by utilizing a synchronous clock. In contrast, one can get away from the synchronous setting and sample the signal only when there is an event. This leads to an alternative sampling paradigm that is known by, Asynchronous [2]–[5], Irregular [6], [7], Event-Driven [8], Time-Encoded [9], Send-on-Delta Sampling [10], [11] which has been widely studied due to its advantage of being power efficient.

Existing works on the event-driven sampling or `EDS` are predominantly concentrated on bandlimited signal classes. Several papers in the recent years have started to consider time-domain sparse signals [12]–[16]. Apart from the bandlimited and sparse signal classes, another class of signals that plays a pivotal role in application areas is that of Fourier-domain sparse signals. Such signals take the form of a sparse mixture of sinusoids in the time-domain and the field of frequency or spectral estimation is devoted to the recovery of sinusoidal parameters [17], [18]. Despite their prevalence, such signals have not been considered in the literature. This can be attributed to various reasons. Firstly, sinusoidal mixtures can be interpreted as a specific case of bandlimited signals. However, this viewpoint leads to sub-optimal recovery as it does not leverage the parametric structure of the sinusoids. Secondly, algorithmic approaches for time-decoding [9] do not straightforwardly translate to sparse or parametric signals [12]–[16]. In this context, the consideration of sparse signals is only very recent and it is natural to consider time-domain sparse signals as a first prototype example. Finally, `EDS` ADCs are still not mainstream yet and hence, such hardware has not been confronted with problems such as direction-of-arrival estimation which intrinsically requires sinusoidal estimation.

The work of the authors is supported by the UK Research and Innovation council's FLF Program "Sensing Beyond Barriers via Non-Linearities" (MRC Fellowship award no. MR/Y003926/1). Further details on Unlimited Sensing and upcoming materials on *reproducible research* are available via `https://bit.ly/USF-Link`.

Contributions. In this paper, we present an event-driven frequency estimation algorithm called **`ED-FreEst`**, that directly extracts the frequency component from its time-encoded measurements. Compared to the sequential reconstruction (*i.e.*, signal recovery followed by frequency estimation), this allows for high-resolution frequency estimation with lower sampling rate (trigger times). Our main contributions are as follows.

- We propose a novel algorithm that directly retrieves the spectral information from its time-encoded measurements. Our algorithmic machinery is based on deconstructing non-linear multidimensional optimization problem into a sequence of one-dimensional optimization problems, which results in a computationally efficient implementation.
- Since practical validation of `EDS` has been rarely reported in previous works, the validity of theoretical algorithms in real-world scenarios remains unknown. To this end, we build `EDS` hardware utilizing asynchronous sigma-delta modulators (ASDM) to validate our approach, demonstrating its performance in realistic settings.

II. Event-Driven Sampling of Multiple Sinusoids

Problem Formulation. The `EDS` scheme used in this paper is depicted in Fig. 1, which represents the amplitude information of the input signal $g(t)$ as a time sequence $\{t_n\}_{n\in\mathbb{Z}}$. The bounded input signal $g(t), |g(t)| \leqslant c < b$, is shifted by a constant amount $\pm b$ before being fed into the integrator. The bias b ensures that the integrator's output $y(t)$ is a positive (negative) increasing (decreasing) function of time. There are two possible operating modes in steady state. In the first mode, the output of the `EDS` is in state $z(t) = -b$ and the input to the Schmitt trigger increases from $-\delta$ to δ. When the output of the integrator reaches the maximum value δ, a transition of the output signal $z(t)$ from $-b$ to $+b$ is triggered and the feedback changes the sign (becomes negative). In the second mode of operation, the `EDS` is in the state $z(t) = b$ and the integrator output steadily decreases from

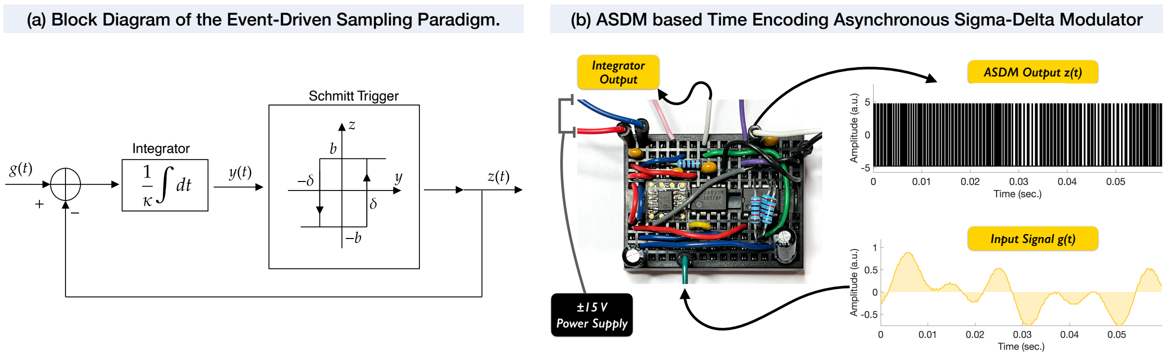

Fig. 1. The block diagram and hardware implementation of the EDS paradigm.

δ to $-\delta$. When the minimum value $-\delta$ is achieved, $z(t)$ will reverse to $-b$. Therefore, while the transition times of the output $z(t)$ are non-uniformly spaced, the modulus of the output signal $z(t)$ remains constant, *i.e.*$|z(t)| = b$. As a result, a transition of the output from $-b$ to b or vice-versa takes place every time the integrator output reaches the triggering threshold δ or $-\delta$. Hence, the EDS maps amplitude information into timing information via a signal-dependent sampling paradigm.

In this paper, we focus on the sum-of-sinusoids input

$$g(t) = \sum\nolimits_{k=0}^{K-1} c_k e^{\jmath \omega_k t}, \ t \in [0, \tau] \tag{1}$$

which generates an encoded time sequence $\{t_n\}_{n=0}^{N}$. Our goal is to retrieve the signal parameters $\{c_k, \omega_k\}_{k=0}^{K-1}$ from the time sequence $\{t_n\}_{n=0}^{N}$ at the output of the EDS.

Sampling Conditions. We show that the recovery is possible via a time-decoding machine, that is, the input signal $g(t)$ can be recovered from $\{t_n\}_{n=0}^{N}$ without any loss of information.

By design (see Fig. 1), the sequence of trigger times $\{t_n\}_{n=0}^{N}$ is generated by the recursive equation

$$\int_{t_n}^{t_{n+1}} g(t)dt = (-1)^n \left[-b\left(t_{n+1} - t_n\right) + 2\kappa\delta\right]. \tag{2}$$

Without any loss of generality, a simple version of the EDS will be used assuming $|g(t)| \leqslant c < 1, \forall t \in [0, \tau]$, $b = 1$ and $\kappa = 1/2$, which leads to the simplified equations,

$$\int_{t_n}^{t_{n+1}} g(t)dt = (-1)^n \left[\delta - (t_{n+1} - t_n)\right] \tag{3}$$

where $\sum_{k=0}^{K-1} |c_k| < 1$. From (3), we have the following result:

Proposition 1. *For an arbitrary bounded signal $g(t)$ with $|g(t)| \leqslant c < 1, \forall t \in [0, \tau]$, the distance between consecutive trigger times t_n and t_{n+1} is bounded by*

$$\frac{\delta}{1+c} \leqslant t_{n+1} - t_n \leqslant \frac{\delta}{1-c}, \quad n \in [0, N-1]. \tag{4}$$

Proof. With $|g(t)| \leqslant c < 1$, we know that $-c(t_{n+1} - t_n) \leqslant \int_{t_n}^{t_{n+1}} g(t)dt \leqslant c(t_{n+1} - t_n)$. By replacing the integral in (3) and solving for $t_{n+1} - t_n$, we obtain the desired result. $\square$

The indicator function on domain $\mathcal{D}$ is denoted by $\mathbb{1}_{\mathcal{D}}$. The input signal $g(t)$ is bandlimited to $[-\Omega, \Omega]$ where $\Omega = \max_k |\omega_k|$. Let the operator $\mathcal{A}(\cdot)$ be defined as

$$\mathcal{A}(t) = \sum\nolimits_{n \in \mathbb{Z}} g(s_n) f_n(t) \tag{5}$$

where $f_n(t) \stackrel{\text{def}}{=} \left(h_\Omega * \mathbb{1}_{[t_n, t_{n+1}]}\right)(t)$, $h_\Omega(t) = \sin(\Omega t)/\pi t$ and $s_n = (t_{n+1} + t_n)/2$. Denote by $g_l(t), t \in [0, \tau]$ a sequence of bandlimited functions defined by the recursion

$$g_{l+1} = g_l + \mathcal{A}(g - g_l), \quad l \in \mathbb{N} \tag{6}$$

with the initial condition $g_0 = \mathcal{A}(g)$ ($g_l = g_l(t)$). Then, the signal $g(t)$ can be recovered from its associated trigger times $\{t_n\}_{n=0}^{N}$, as $\lim_{l \to \infty} g_l(t) = g(t)$, provided that [9],

$$\delta < \frac{(1-c)\pi}{\Omega}, \quad \Omega = \max_k |\omega_k|. \tag{7}$$

Once $g(t)$ is recovered, $\{\omega_k\}_{k=0}^{K-1}$ can be retrieved from a sequence of uniform samples $\{g(mT)\}_{m=0}^{M-1}$ via Prony's method [17], provided that $T \leqslant \frac{\pi}{\Omega}$. With $\{\omega_k\}_{k=0}^{K-1}$ known, $\{c_k\}_{k=0}^{K-1}$ can be obtained via least-squares.

III. ED-FreEst: Event-Driven Frequency Estimation

In this paper, instead of performing sequential reconstruction, *viz.* , recover $g(t)$ from $\{t_n\}_{n=0}^{N}$ first and estimate $\{c_k, \omega_k\}_{k=0}^{K-1}$ later, our goal is to achieve frequency estimation directly from the time sequence $\{t_n\}_{n=0}^{N}$.

Our starting point is the non-uniform measurements from the output of the integrator. Combining (1) and (3), we have,

$$y[n] = \int_{t_n}^{t_{n+1}} g(t)dt \stackrel{(1)}{=} \sum\nolimits_{k=0}^{K-1} \underline{c}_k \left(e^{\jmath\omega_k t_{n+1}} - e^{\jmath\omega_k t_n}\right) \tag{8}$$

where $n = 0, \cdots, N-1$ and $\underline{c}_k = \frac{c_k}{\jmath\omega_k}, k = 0, \cdots, K-1$. Notice that, $\{y[n]\}_{n=0}^{N-1}$ can be obtained from $\{t_n\}_{n=0}^{N}$,

$$y[n] \stackrel{(3)}{=} (-1)^n \left[\delta - (t_{n+1} - t_n)\right]. \tag{9}$$

Direct Frequency Estimation from EDS Samples. Given $\{y[n]\}_{n=0}^{N-1}$, we consider estimating the unknown parameters by minimizing the below quadratic function

$$\mathcal{J}(\mathbf{c}, \boldsymbol{\omega}) = \sum_{n=0}^{N-1} \left| y[n] - \sum_{k=0}^{K-1} \underline{c}_k (e^{\jmath\omega_k t_{n+1}} - e^{\jmath\omega_k t_n}) \right|^2 \tag{10}$$

Algorithm 1 Event-Driven Frequency Estimation

Input: Time sequence $\{t_n\}_{n=0}^{N}$.
Compute the samples $\{y[n]\}_{n=0}^{N-1}$ via (9).
Compute the parameter initialization $\{c_k^{[0]}, \omega_k^{[0]}\}_{k=0}^{K-1}$.
for `l = 1` to `max. iterations` **do**
  for `m = 1` to `K` **do**
    Compute the residue $\mathbf{y}_m$ via (11).
    Update $\{c_k^{[l]}, \omega_k^{[l]}\}$ via (13) and (14).
  end for
  if (16) holds **then**
    `Terminate all loops;`
  end if
end for
Output: The reconstructed signal $g(t)$.

where $\mathbf{c} = [c_0, \cdots, c_{K-1}]^\top$ and $\boldsymbol{\omega} = [\omega_0, \cdots, \omega_{K-1}]^\top$, where $(\cdot)^\top$ denotes the transpose. Minimizing $\mathcal{J}(\mathbf{c}, \boldsymbol{\omega})$ in (10) is equivalent to maximizing the likelihood when the measurements $y[n]$ is corrupted by white Gaussian noise. Even when the noise is not white, minimizing $\mathcal{J}(\mathbf{c}, \boldsymbol{\omega})$ still results in an excellent statistical accuracy as reported in [19]–[22].

The minimization on $\mathcal{J}(\mathbf{c}, \boldsymbol{\omega})$ with respect to the unknown parameters is a highly non-linear optimization problem. Below, we present a novel algorithm to obtain the frequency parameter estimates in an iterative orthogonal matching pursuit (OMP) manner. Before we state our method, let us introduce the following notations. Let $\mathbf{g}(\omega_k) = [e^{\jmath\omega_k t_{n+1}} - e^{\jmath\omega_k t_n}]_{n=0}^{N-1}$, $\mathbf{y} = [y[0], \cdots, y[N-1]]^\top$, and $\mathbf{c} = [\underline{c}_0, \cdots, \underline{c}_{K-1}]^\top$. Denote

$$\mathbf{y}_m = \mathbf{y} - \sum\nolimits_{k \neq m} \widehat{c}_k \mathbf{g}(\widehat{\omega}_k) \tag{11}$$

where $\{\widehat{c}_k, \widehat{\omega}_k\}_{k=0,k\neq m}^{K-1}$ are known. Then, (10) becomes

$$\mathcal{J}(c_m, \omega_m) = \|\mathbf{y}_m - c_m \mathbf{g}(\omega_m)\|_2^2 \tag{12}$$

where $\|\cdot\|$ denotes the ℓ_2 norm. Notice that, minimizing (12) on c_m, ω_m can be decoupled separately, where the estimate $\widehat{c}_m$ of c_m can be characterized by the estimate $\widehat{\omega}_m$ of ω_m as

$$\widehat{c}_m = \left.\frac{\langle \mathbf{g}(\omega_m), \mathbf{y}_m \rangle}{\|\mathbf{g}(\omega_m)\|_2^2}\right|_{\omega_m = \widehat{\omega}_m} \tag{13}$$

where $\langle \cdot, \cdot \rangle$ denotes the inner product. Hence, with (13), the estimate $\widehat{\omega}_m$ of ω_m is given by

$$\widehat{\omega}_m = \arg\max\nolimits_{\omega_m} |\langle \mathbf{u}(\omega_m), \mathbf{y}_m \rangle| \tag{14}$$

where $\mathbf{u}(\omega_m) = \frac{\mathbf{g}(\omega_m)}{\|\mathbf{g}(\omega_m)\|_2}$. Notice that, $\widehat{\omega}_m$ is obtained as the location of the dominant peak of the magnitude of the cross-correlation between $\mathbf{u}(\omega_m)$ and $\mathbf{y}_m$, which can be efficiently solved via 1-D optimization methods, such as Golden section search algorithm, dichotomic search approach, etc.

Given initial parameter estimates, we can iteratively refine each frequency component $\{c_m, \omega_m\}$ in an orthogonal matching pursuit (OMP) manner: in m-th iteration, we compute the residue $\mathbf{y}_m$ via (11) by excluding the remaining frequency components $\{\widehat{c}_k, \widehat{\omega}_k\}_{k=0,k\neq m}^{K-1}$. Then, the parameter estimates $\{\widehat{c}_m, \widehat{\omega}_m\}$ can be updated via (13) and (14). As a result, the non-trivial multi-dimensional minimization problem can be transformed into a series of 1-D optimization problems, allowing for an efficient and accurate algorithm implementation.

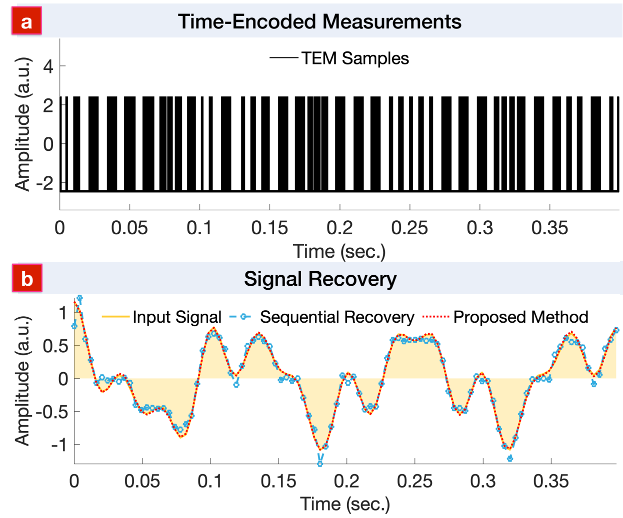

Fig. 2. Numerical Experiment: (a) Time-encoded samples and (b) signal recoveries. The frequencies to be estimated are $f_k = [8, 20, 30]$Hz. The sampling rates are $\bar{f}_s = 10$kHz (sequential reconstruction) and $f_s = 2$kHz (**`ED-FreEst`**). The low sampling rate results in distortion in sequential reconstruction ($\mathcal{E}_2(\mathbf{f}_k, \bar{\mathbf{f}}_k) = 6.43 \times 10^{-1}$), yet **`ED-FreEst`** provides an accurate recovery with $\mathcal{E}_2\left(\mathbf{f}_k, \widetilde{\mathbf{f}}_k\right) = 1.94 \times 10^{-3}$.

Convergence and Algorithm Initialization. We design a robust parameter initialization strategy to ensure a fast convergence speed of the proposed event-driven frequency estimation algorithm (**`ED-FreEst`**). From (14), it suffices to show that the cross-correlation function $\mathcal{C}(\omega) = |\langle \mathbf{u}(\omega), \mathbf{y}_m \rangle|$ attains local maxima at $\omega = \omega_k, k = 0, \cdots, K-1$. Therefore, a deterministic parameter initialization can be obtained by evaluating $\mathcal{C}(\omega)$ on a frequency grid and pick the K most prominent peaks ("`islocalmax`" function in `Matlab`) [22].

The algorithm is bound to converge to at least some local minimum point [23], since the minimization results in

$$\mathcal{J}(\widehat{c}_m, \widehat{\omega}_m) \overset{(14)}{\leqslant} \mathcal{J}(\widehat{c}_{m+1}, \widehat{\omega}_{m+1}). \tag{15}$$

The convergence speed depends on the frequency spacing of the signal $g(t)$. If the separation between any two frequencies is sufficiently large, the algorithm converges in a few steps. As the frequency separation becomes closer, the convergence speed becomes slower. We keep iterating the algorithm until the relative change of the cost function $\mathcal{J}(\mathbf{c}, \boldsymbol{\omega})$ between two consecutive parameter estimates is sufficiently small, *i.e.*,

$$\mathcal{J}\left(\mathbf{c}^{[l]}, \boldsymbol{\omega}^{[l]}\right) - \mathcal{J}\left(\mathbf{c}^{[l+1]}, \boldsymbol{\omega}^{[l+1]}\right) \leqslant \epsilon \tag{16}$$

where $l = 0, \cdots, l_{\max}$ and ϵ is a positive value. The procedure is summarized in Algorithm 1.

TABLE I

NUMERICAL AND HARDWARE EXPERIMENTAL PARAMETERS AND PERFORMANCE EVALUATION.

Figure	N	f_s	$\bar{f}_s$	κ	δ	b	$\|g\|_\infty$	f_k	$\widetilde{f}_k$	$\bar{f}_k$	$\mathcal{E}_2(\mathbf{f}_k, \widetilde{\mathbf{f}}_k)$	$\mathcal{E}_2(\mathbf{f}_k, \bar{\mathbf{f}}_k)$	$\mathcal{E}_2(\mathbf{g}, \widetilde{\mathbf{g}})$	$\mathcal{E}_2(\mathbf{g}, \bar{\mathbf{g}})$
		(kHz)	(kHz)					(Hz)	(Hz)	(Hz)				
Numerical Experiments														
—	387	7.50	300.00	4.38×10^{-4}	1.50	1.80	0.60	15.0	15.01	15.00	1.72×10^{-4}	2.20×10^{-8}	9.05×10^{-6}	7.31×10^{-6}
—	345	1.50	30.00	4.38×10^{-4}	1.50	1.80	0.60	15.0	15.00	14.99	1.86×10^{-5}	4.97×10^{-5}	9.82×10^{-7}	1.58×10^{-2}
—	521	6.00	300.00	4.38×10^{-4}	1.50	2.40	1.20	$[8.0, 20.0, 30.0]$	$[8.04, 19.98, 30.11]$	$[7.99, 19.96, 29.97]$	4.34×10^{-3}	9.03×10^{-4}	2.11×10^{-4}	4.24×10^{-6}
Fig. 2	636	2.00	10.00	4.38×10^{-4}	1.50	2.40	1.20	$[8.0, 20.0, 30.0]$	$[8.01, 19.93, 30.02]$	$[7.26, 18.88, 29.62]$	1.94×10^{-3}	6.43×10^{-1}	1.41×10^{-4}	6.26×10^{-3}
Hardware Experiments														
—	189	15.62	500.00	5.78×10^{-4}	0.95	4.73	5.17	37.0	37.03	36.98	1.16×10^{-3}	3.60×10^{-4}	8.53×10^{-4}	2.08×10^{-3}
—	204	15.62	500.00	5.54×10^{-4}	0.95	4.73	5.17	57.0	57.01	56.96	5.20×10^{-5}	1.58×10^{-3}	8.26×10^{-4}	2.58×10^{-3}
—	214	15.62	500.00	5.46×10^{-4}	0.95	4.73	5.08	77.0	76.85	77.04	2.17×10^{-2}	1.49×10^{-3}	1.54×10^{-3}	2.58×10^{-3}
Fig. 3	308	15.62	500.00	4.18×10^{-4}	0.95	4.72	4.60	$[13.0, 59.0, 97.0]$	$[14.09, 58.56, 97.80]$	$[19.17, 55.75, 97.98]$	6.71×10^{-1}	1.65×10^{1}	6.08×10^{-4}	1.55×10^{-3}

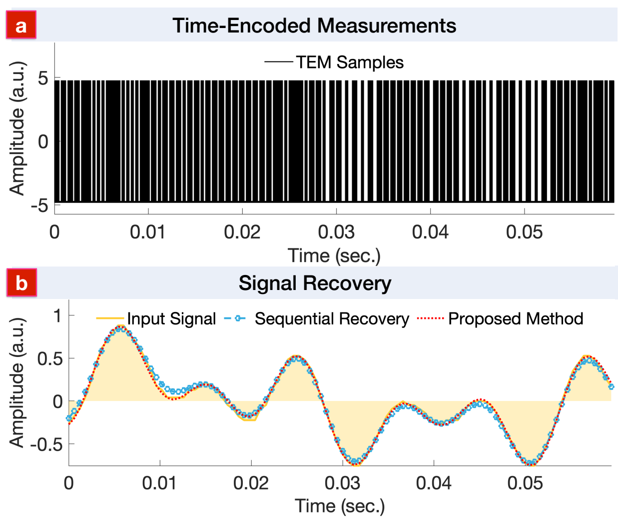

Fig. 3. Hardware Experiment: (a) Time-encoded samples and (b) signal recoveries. The frequencies to be estimated are $f_k = [13, 59, 97]$Hz. The sampling rates are $\bar{f}_s = 500$kHz (sequential reconstruction) and $f_s = 15.62$kHz (**ED-FreEst**). Despite 32× downsampling, **ED-FreEst** still achieves an accurate signal recovery as well as frequency estimation ($\mathcal{E}_2\left(\mathbf{f}_k, \widetilde{\mathbf{f}}_k\right) = 6.71 \times 10^{-1}$), validating its performance and practical utility.

IV. NUMERICAL AND HARDWARE EXPERIMENTS

The overarching goal of our experiments is to push the sampling rate on trigger times and duration of the proposed **ED-FreEst** approach. In particular, through a series of 8 experiments, we show that the frequency information can be directly retrieved from the time-encoded measurements, utilizing an asynchronous sigma–delta modulation implementation, providing a factor of 30× improvement on sampling rate in real-world scenarios. This also serves as a validation of our method (Algorithm 1) presented in Section II. We compare the proposed method to the sequential reconstruction via (5) and (6) to demonstrate the algorithm performance. For a sum of sinusoids g as defined in (1), we use $\widetilde{g}$ ($\widetilde{f}_k$) and $\bar{g}$ ($\bar{f}_k$) to denote the signal recovery (frequency estimates) by the proposed method and sequential reconstruction, respectively. We use the mean-squared error, $\mathcal{E}_2\left(\mathbf{f}_k, \widetilde{\mathbf{f}}_k\right) = \frac{1}{K}\sum_{k=0}^{K-1} |f_k - \widetilde{f}_k|^2$ to evaluate the frequency estimation error. We use $\mathcal{E}_2(\mathbf{g}, \widetilde{\mathbf{g}}) = \frac{1}{M}\sum_{m=0}^{M-1} |g[m] - \widetilde{g}[m]|^2$ to measure signal recovery error. Experimental parameters such as, ground-truth frequencies f_k, dynamic range, sampling rate f_s (**ED-FreEst** method), sampling rate $\bar{f}_s$ (sequential reconstruction), bias b, among others are tabulated in the first row of Table I, respectively.

Numerical Experiments. In noiseless scenarios, numerical experiments show that the proposed method gives rise to an accurate signal recovery and frequency estimation, offering 30-50× reducing on sampling rate. In particular, we observe that the sequential reconstruction method compromises estimation accuracy at $\bar{f}_s = 10$kHz as illustrated in Table I and Fig. 2. **ED-FreEst** achieves higher frequency estimation precision at a lower sampling rate of 2kHz, using dichotomic search for (14).

Hardware Experiments. To assess the practicability and robustness of our method, we further perform hardware experiments based on asynchronous sigma–delta modulator that implements the EDS pipeline described in Fig. 1. The sum of sinusoids is generated by TG5011A signal generators via amplitude modulation (AM). The experimental parameters and results are summarized in Table I.

We conduct experiments in both single- and multiple-sinusoids case. The time-encoded samples and corresponding signal recoveries are plotted in Fig. 3. As shown in Fig. 3 (b), the sequential reconstruction is sensitive to the sampling rate ($\bar{f}_s = 500$kHz), yielding distortion around $t = 0.01$ sec. This reconstruction error eventually results in error on frequency estimation with $\mathcal{E}_2\left(\mathbf{f}_k, \bar{\mathbf{f}}_k\right) = 1.65 \times 10^1$ and $\mathcal{E}_2(\mathbf{g}, \bar{\mathbf{g}}) = 1.55 \times 10^{-3}$. Despite a much lower sampling rate on trigger times with $f_s = 15.62$kHz, **ED-FreEst** achieves a more accurate frequency estimation as well as signal recovery with $\mathcal{E}_2\left(\mathbf{f}_k, \widetilde{\mathbf{f}}_k\right) = 6.71 \times 10^{-1}$ and $\mathcal{E}_2(\mathbf{g}, \widetilde{\mathbf{g}}) = 6.08 \times 10^{-4}$. These hardware experiments effectively demonstrate the practical utility and robust performance of **ED-FreEst** algorithm in real-world applications.

V. CONCLUSION

As an alternative to capturing signal amplitude at uniform time instances, EDS scheme only samples the signal non-uniformly, converting the amplitude information into a sequence of time stamps. In this paper, we focus on the sums of sinusoids signal and design a novel algorithm that allows for a direct frequency estimation from its time-encoded samples. This reduces the sampling rate on trigger times and provide a high-resolution frequency estimation. We go beyond numerical experiments and also provide a hardware validation of our approach, thus bridging the gap between theory and practice, while corroborating the potential benefits of our method.

REFERENCES

[1] C. Shannon, "Communication in the presence of noise," *Proc. IRE*, vol. 37, no. 1, pp. 10–21, Jan. 1949.

[2] J. Das and P. Sharma, "Some asynchronous pulse-modulation systems," *Electron Lett*, vol. 3, no. 6, p. 284, 1967.

[3] T. Hawkes and P. Simonpieri, "Signal coding using asynchronous delta modulation," *IEEE Trans. Commun.*, vol. 22, no. 5, pp. 729–731, May 1974.

[4] A. M. Bruckstein and Y. Y. Zeevi, "Analysis of "integrate-to-threshold" neural coding schemes," *Biol. Cybernet.*, vol. 34, no. 2, pp. 63–79, 1979.

[5] E. Roza, "Analog-to-digital conversion via duty-cycle modulation," *IEEE Trans. Circuits Syst. II*, vol. 44, no. 11, pp. 907–914, 1997.

[6] H. G. Feichtinger and K. Gröchenig, "Irregular sampling theorems and series expansions of band-limited functions," *J. Math. Anal. Appl.*, vol. 167, no. 2, pp. 530–556, Jul. 1992.

[7] K. Gröchenig, "A discrete theory of irregular sampling," *Linear Algebra Appl*, vol. 193, pp. 129–150, Nov. 1993.

[8] Y. Tsividis, "Event-driven data acquisition and digital signal processing—a tutorial," *IEEE Transactions on Circuits and Systems II: Express Briefs*, vol. 57, no. 8, pp. 577–581, Aug. 2010.

[9] A. Lazar and L. Toth, "Perfect recovery and sensitivity analysis of time encoded bandlimited signals," *IEEE Trans. Circuits Syst. I*, vol. 51, no. 10, pp. 2060–2073, Oct. 2004.

[10] M. Miskowicz, "Send-on-delta concept: An event-based data reporting strategy," *Sensors*, vol. 6, no. 1, pp. 49–63, Jan. 2006.

[11] B. A. Moser and M. Lunglmayr, "On quasi-isometry of threshold-based sampling," *IEEE Trans. Sig. Proc.*, vol. 67, no. 14, pp. 3832–3841, Jul. 2019.

[12] A. Can, E. Sejdić, and L. Chaparro, "Asynchronous sampling and reconstruction of sparse signals," in *Proc. of the European Sig. Proc. Conf. (EUSIPCO)*, 2012.

[13] R. Alexandru and P. L. Dragotti, "Reconstructing classes of non-bandlimited signals from time encoded information," *IEEE Trans. Sig. Proc.*, vol. 68, pp. 747–763, 2020.

[14] S. Rudresh, A. J. Kamath, and C. Sekhar Seelamantula, "A time-based sampling framework for Finite-Rate-of-Innovation signals," in *Proc. IEEE Int. Conf. Acoust., Speech, Sig. Proc.*, May 2020.

[15] H. Naaman, S. Mulleti, and Y. C. Eldar, "FRI-TEM: Time encoding sampling of finite-rate-of-innovation signals," *IEEE Trans. Sig. Proc.*, vol. 70, pp. 2267–2279, 2022.

[16] D. Florescu and A. Bhandari, "Time encoding of sparse signals with flexible filters," in *Intl. Conf. on Sampling Theory and Applications (SampTA)*. IEEE, Jul. 2023.

[17] P. Stoica and R. L. Moses, *Spectral analysis of signals*, 1st ed. Pearson Prentice Hall, 2005.

[18] E. Robinson, "A historical perspective of spectrum estimation," *Proc. IEEE*, vol. 70, no. 9, pp. 885–907, Sep. 1982.

[19] J. Li and P. Stoica, "Efficient mixed-spectrum estimation with applications to target feature extraction," *IEEE Trans. Sig. Proc.*, vol. 44, no. 2, pp. 281–295, Feb. 1996.

[20] J. Li and R. Wu, "An efficient algorithm for time delay estimation," *IEEE Trans. Sig. Proc.*, vol. 46, no. 8, pp. 2231–2235, Aug. 1998.

[21] Y. Li, R. Guo, T. Blu, and H. Zhao, "Generic FRI-based DOA estimation: A model-fitting method," *IEEE Trans. Sig. Proc.*, vol. 69, pp. 4102–4115, 2021.

[22] R. Guo, Y. Li, T. Blu, and H. Zhao, "Vector-FRI recovery of multi-sensor measurements," *IEEE Trans. Sig. Proc.*, vol. 70, pp. 4369–4380, 2022.

[23] V. G. Karmanov, *Mathematical programming*. Mir Publishers, 1989.